

# O-RAN xApps Conflict Management using Graph Convolutional Networks

Maryam Al Shami, *WIE Member, IEEE*, Jun Yan, *Member, IEEE*, and Emmanuel Thepie Fapi

**Abstract**—Open Radio Access Network (O-RAN) adopts a flexible, open, and virtualized structure with standardized interfaces, reducing dependency on a single supplier. Conflict management in O-RAN refers to the process of identifying and resolving conflicts between network applications. xApps are applications deployed at the RAN Intelligent Controller (RIC) that leverage advanced AI/ML algorithms to make dynamic decisions for network optimization. The lack of a unified mechanism to coordinate and prioritize the actions of different applications can create three types of conflicts (direct, indirect, and implicit). In our paper, we introduce a novel data-driven GCN-based method called Graph-based xApps Conflict and Root Cause Analysis Engine (GRACE) based on Graph Convolutional Network (GCN). It detects three types of conflicts (direct, indirect, and implicit) and pinpoints the root causes (xApps). GRACE captures the complex and hidden dependencies among the xApps, the controlled parameters, and the KPIs in O-RAN to detect possible conflicts. Then, it identifies the root causes (xApps) contributing to the detected conflicts. The proposed method was tested on highly imbalanced datasets where the number of conflict instances ranges from 40% to 10%. The model is tested in a setting that simulates real-world scenarios where conflicts are rare to assess its performance and generalizability. Experimental results demonstrate an exceptional performance, achieving a high F1-score greater than 98% for all the case studies.

**Index Terms**—5G Networks and Beyond, O-RAN, Quality of Service, Conflict Management, xApps, Graph Neural Network, Root Cause Analysis, Key Performance Indicators.

## I. INTRODUCTION

THE O-RAN represents a paradigm shift in how mobile networks are developed and operated. Traditionally, mobile networks are designed such that each layer of the cellular protocol stack is implemented as a black box with a limited number of vendors. This limits RAN reconfigurability, and coordination among nodes, making it difficult to deploy and integrate equipment from multiple vendors [1]. Motivated by this, O-RAN is introduced to decouple the network’s hardware and software components. Thus, promoting interoperability, openness, and flexibility in the design and deployment of RAN components [1].

Service Management and Orchestration (SMO) and Radio Intelligent Controller (RIC) are two important components of the O-RAN architecture. The SMO is responsible for the overall orchestration, management, and automation of the O-RAN [1]. The RIC serves as a platform to deploy applications that use machine learning models to predict network behavior, detect anomalies, and enhance decision-making capabilities [2]. The intelligent, data-driven control with the RICs is provided through two logical controllers: Non-Real Time RIC (Non-RT RIC) and the Near-RT RIC (Near-RT RIC) [3]. These

two RICs provide a platform to host third-party applications that could be powered by machine learning to orchestrate the RAN for specific tasks [4]. They differ in terms of the functions they perform and the timescales over which they operate.

In this context, xApps (eXtended Applications) are software applications designed to run on the Near-RT RIC. These applications are intended to make real-time, fast-paced decisions that immediately impact day-to-day operations and user experiences. xApps play a key role in ensuring Quality of Service (QoS) by providing flexible and dynamic control over various aspects of the network behavior. This includes load balancing [5], interference management [6], and handover optimization [7], [8]. The autonomous operation of xApps managed by different third-party vendors makes them susceptible to conflicts. Each xApp has its own objective and decision-making process. This will introduce new challenges as these applications independently interact with the network environment. The actions of one or more applications could potentially adversely impact the objectives of the others as they share the same network resources or parameters [9]–[11].

Existing solutions leverage AI/ML approaches to address various O-RAN QoS problems. In [12], the authors develop three xApps for Deep Reinforcement Learning (DRL)-based control of RAN slicing, scheduling, and online model training using CoO-RAN. A user-specific O-RAN traffic steering framework for intelligent handovers is unfolded in [13]. The system combines a random ensemble mixture, a conservative Q-learning algorithm, and a convolutional neural network architecture. The paper [14] addresses mobility load balancing and optimization using a random subspace Bayesian additive regression tree and interior point policy optimization for a seamless user experience. In [15], the authors introduce a DRL-based radio resource management solution for RAN slicing with guaranteed service-level agreement.

Other studies seek to detect or predict the occurrences of conflicts in O-RAN. In [16], a team deep Q-learning algorithm for resource allocation is disclosed to mitigate xApps conflicts in O-RAN. In [17], a bargaining game-theoretic approach is introduced along with a standardized Conflict Mitigation System (CMS) and independent controllers. This work is further improved in [18]. They use a cooperative game theory to optimize the conflicting parameters while maximizing the number of xApps that meet QoS requirements. In [19], a Deep Q-Network and a multi-headed multilayer perceptron network model are presented. The method distills knowledge from multiple xApps to train a single model retaining the capabilities of previous xApps.

Other works address the xApps conflict management using graph-based approaches. The authors in [20] aims to detect, characterize, and mitigate conflicts among applications in O-RAN. Accordingly, they combine hierarchical graphs with statistical knowledge of applications to find dependencies between control parameters and Key Performance Measurements. In [21], the paper suggests using GraphSAGE for reconstructing and labeling conflict graphs in O-RAN. It captures the hidden dependencies between xApps, parameters, and KPIs. Then, graph labeling is performed to identify the different types of conflicts based on well-defined, graph-based definitions.

Understanding the complex and intricate dependencies between the xApps, the controlled parameters, and the KPIs is imperative to address the xApp conflict RCA. It allows us to detect the different types of conflicts in real time and derive the contributing root causes (xApps) for proactive maintenance. In the previously mentioned non-graph-based approaches, there is still a substantial limitation in their capacity to effectively capture and model dependencies within complex data structures. The proposed method in [21] leverages GraphSAGE to effectively capture the dependencies within the data. However, it still falls short of fully accounting for the imbalanced nature of the datasets in practical life scenarios, as these conflicts are rare to happen. Addressing this limitation is crucial for enhancing the robustness and generalizability of the proposed approach in real-world applications. Accordingly, we propose GRACE, a GCN-based method that is capable of handling highly imbalanced datasets with up to 10% conflicts. It detects the xApps conflicts (direct, indirect, and implicit) and identifies their root causes (xApps) for future mitigation strategies.

Our technical contributions are as follows:

- We propose a 5G O-RAN xApps conflict detection with a root cause analysis method using Graph Convolutional Networks (GCNs). This allows us to capture the complex and hidden dependencies between the xApps, parameters, and KPIs in the network to detect xApps conflicts (direct, indirect, and implicit).
- We leverage a binary state-based GCN structure to map and explain the complex relationships. This ensures the generalizability of the proposed solution, which can be extended to other networks. This structure along with the detections are the key inputs for the root cause analysis.
- We use the focal loss function in the model training. This allows the model to handle highly imbalanced datasets. The model generalizes effectively to unseen data while maintaining an F1 score greater than 98%.

The remainder of this paper is structured as follows. Section II presents the problem formulation, clearly defining the research question and outlining the scope and objectives of the study. Section III describes the proposed system model. Section IV details the evaluation metrics, the experimental setup, and the interpretation of the results. Section V concludes this paper.

## II. PRELIMINARIES

Conflict management is a crucial aspect of O-RAN, ensuring different applications operate harmoniously within the network. The conflicts can be categorized into three types: Direct, indirect, and implicit conflict [20], [22], [23]. Fig. 1 illustrates the various types of conflicts in the network.

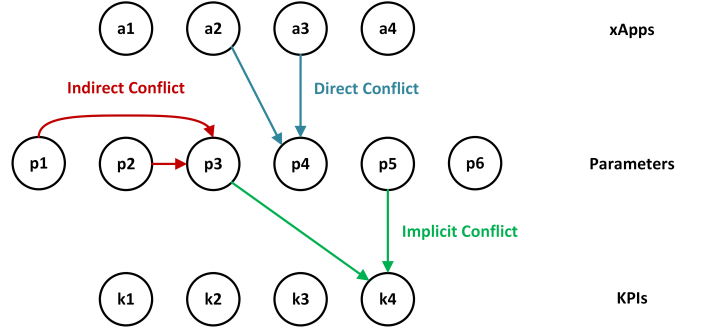


Fig. 1. The xApps conflicts examples.

Direct conflicts arise when multiple applications attempt to modify or request different settings for the same network parameter simultaneously. These conflicts are easily noticeable and can result in immediate service degradation, unstable performance, or even network failures if not promptly addressed. For example, two xApps might attempt to adjust the transmission power of the same cell simultaneously. In particular, one xApp seeks to increase power for better coverage, while the other aims to reduce it to minimize interference with neighboring cells.

Indirect conflicts are not immediately visible, but the interdependencies between the parameters and resources involved can be observed. These conflicts occur when multiple applications modify a set of parameters that directly affect the values of other parameters. They are subtler than direct conflicts and may result in unintended negative effects. For instance, one xApp may optimize load balancing by redistributing traffic across various cells, while another xApp is adjusting handover parameters to enhance mobility performance. Although these actions are independent, the resulting traffic shifts could disrupt the handover process or increase congestion in certain cells, leading to a degraded user experience.

Implicit conflicts transpire when multiple xApps make control decisions that target different optimization objectives, which interfere with one another. These conflicts are not directly observable. They depend on intrinsic relationships between control parameters and observable Key Performance Indicators (KPIs). They are more abstract and arise from differences in how xApps interpret the network's requirements. For instance, one xApp might prioritize energy efficiency by reducing transmission power across several cells to lower consumption. Meanwhile, another xApp seeks to increase power in certain areas to enhance coverage. The conflicting goals, energy efficiency versus coverage, could lead to poor service quality in some areas of the network or result in inefficient power usage.

Grasping the distinctions between these conflicts in O-RAN is crucial for developing resilient, automated networks. The

network must be capable of efficiently handling various optimization goals such as Quality of Service (QoS), coverage, and energy efficiency. Effective conflict management is necessary as a tailored resolution approach to maintain optimal network performance while achieving specific objectives. This process involves detecting, predicting, resolving, and preventing conflicts between the decisions and actions of xApps.

Dealing with xApps in an O-RAN environment brings many critical challenges that need to be addressed. This involves ensuring that multiple xApps can operate simultaneously and complement each other, leading to a well-optimized network. Specifically, there is a lack of coordination and standardization among the various components responsible for RAN control decisions. Moreover, in large, complex, and hierarchical networks, it is impossible to be able to update the conflict management configuration manually. In addition, as multiple conflicting objectives could co-exist, finding a single optimal solution that optimizes all the objectives may not be feasible. This will make it difficult to identify the conflicts along with their root causes to address them with appropriate mitigation strategies [9], [11].

### III. PROPOSED METHOD

We now introduce our proposed solution conflict model. The proposed framework is depicted in Fig. 2. The Near-RT RIC serves as a key point of collection for the xApps states, the values of the controlled parameters data, and KPI metrics. These data are collected leveraging the subscription manager (SM), which is a part of the Near-RT RIC. SM is responsible for handling the xApps subscriptions. It manages which xApps are subscribed to specific events, KPIs, or data sources from the RAN. Additionally, it tracks the active subscriptions and ensures that xApps receive the data they need. To retrieve the list of the activated xApps, the parameters, and the KPIs, we should interact with the RIC platform via the RIC API.

A database is required to store the collected data from the SM in the Near-RT RIC using the messaging infrastructure. Then, the proposed system retrieves the collected data from the database for further processing using a shared data layer. Our proposed solution requires the implementation of a component that converts the collected data into a binary-state dataset as depicted in Fig. 4. In particular, the state of an activated xApp is presented by "1", and a deactivated xApp is represented by "0". Similarly, if the value of a parameter or a KPI is changed from its previous timestamp value, the state is set to "1", otherwise, the state is set to "0".

The proposed solution executes three major tasks, namely Graph Structure Creator (GSC), Graph Anomaly Detector (GAD), and Root Cause Analyst (RCA). The high-level diagram of the solution is illustrated in Fig. 3. In the remainder of this section, we will provide a detailed description of each module in the proposed method, outlining the corresponding steps and functionality.

#### A. Dataset Generation and Conflicts Modeling

We will thoroughly explain the dataset generation and the modeling of the three types of conflict steps. Let  $\mathcal{A}$  be the set

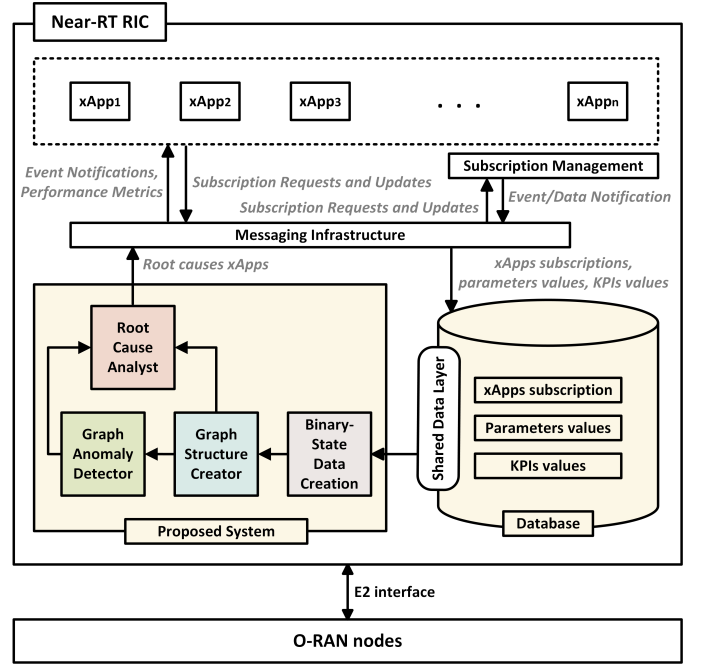


Fig. 2. The proposed framework.

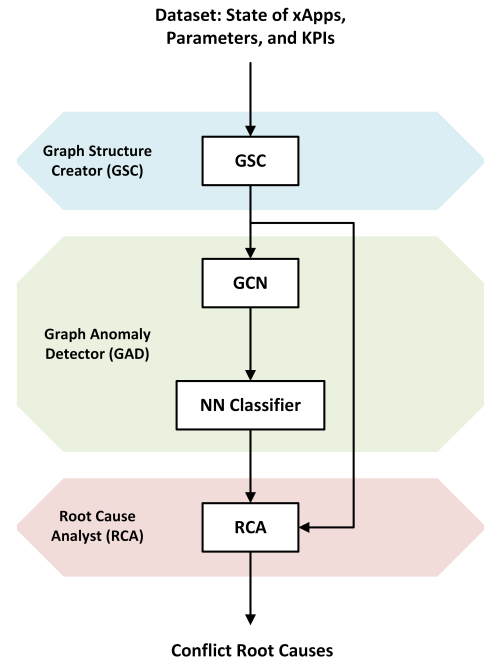


Fig. 3. The high-level diagram of GRACE.

of O-RAN xApps deployed on the Near-RT RIC. Let  $\mathcal{P}$  be the set of parameters that are controlled by applications in  $\mathcal{A}$ , and  $\mathcal{K}$  be the set of observable KPIs.

For each application  $a \in \mathcal{A}$  and parameter  $p \in \mathcal{P}$ , we define a state indicator  $i_{p,a} \in \{0, 1\}$  such that  $i_{p,a} = 1$  if application  $a$  controls parameter  $p$ , and  $i_{p,a} = 0$  otherwise. For each KPI  $k \in \mathcal{K}$  and parameter  $p \in \mathcal{P}$ , we define another state indicator  $j_{k,p} \in \{0, 1\}$  such that  $j_{k,p} = 1$  if parameter  $p$  modifies the value of KPI  $k$ , and  $j_{k,p} = 0$  otherwise. For

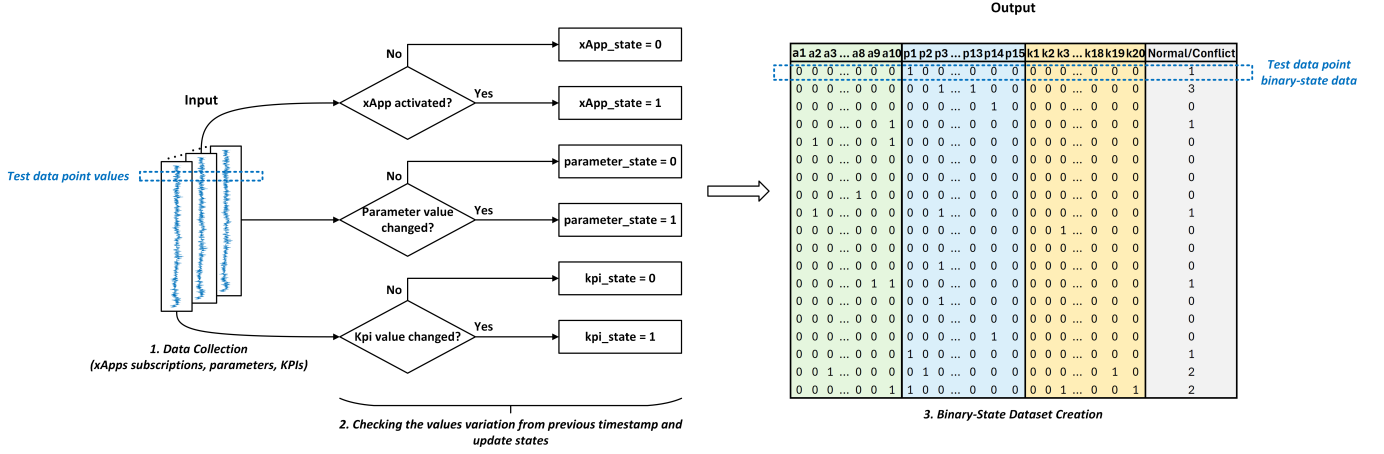


Fig. 4. The binary-state data creation module steps.

each parameter  $p \in \mathcal{P}$ , we create a copy of the set  $\mathcal{P}$  called  $\mathcal{P}'$  and a random parameter  $p' \in \mathcal{P}'$  is chosen such that this parameter is removed from the set  $\mathcal{P}$ . Then, we define another state indicator  $l_{p,p'} \in \{0, 1\}$  such that  $l_{p,p'} = 1$  if parameter  $p$  modifies the value of parameter  $p'$ , and  $l_{p,p'} = 0$  otherwise.

Conflict modeling is performed by randomly selecting elements from each set and mapping them to the elements in the other set without any predetermined pattern or order. This is achieved by shuffling the sets and randomly assigning the elements in the shuffled set to those in the other set. The randomness of the assignment ensures that there is no bias or regularity in the mapping. Each variable has an equal chance of being paired with any other variable from the second set to introduce diversity in the assignments.

Accordingly, five binary-state datasets are generated. Each dataset  $D$  contains a target label column that classifies each data point into one of four distinct classes (0: normal, 1: direct conflict, 2: implicit conflict, and 3: indirect conflict). The first dataset is balanced, and the classes are evenly distributed. The remaining four datasets are generated with different conflict proportions ranging from 40% to 10%. The core idea behind this diversity is to test our model on generated datasets close to real-world scenarios where conflicts are rare.

### B. Graph Structure Creator (GSC)

GSC module is responsible for creating graph-structured data from the binary-state dataset comprising the collected data from the Near-RT RIC (see Fig. 5). A graph-structured data is needed as the GCN-based model operates on graph data. It ingests the binary-state dataset and the number of xApps, parameters, and KPIs as input. The resultant graph-structured data will be the combination of three subgraphs ( $G^{\text{PA}}$ ,  $G^{\text{KP}}$ , and  $G^{\text{P'P}}$ ).

$G^{\text{PA}}$  subgraph: This subgraph  $G^{\text{PA}} = (V^{\text{PA}}, E^{\text{PA}})$  represents the relationships between the applications and the control parameters. Nodes of  $G^{\text{PA}}$  are both the applications and the control parameters, i.e.,  $V^{\text{PA}} = \mathcal{P} \cup \mathcal{A}$ , and edges  $E^{\text{PA}}$  represent whether or not an application is controlling a parameter  $p \in \mathcal{P}$ . Any 2-tuple  $(p, a) \in \mathcal{P} \times \mathcal{A}$  is an edge of

$G^{\text{PA}}$ , i.e.,  $(p, a) \in E^{\text{PA}}$  if and only if parameter  $p$  is directly controlled by an application  $a$ . This will cause a direct conflict.

$G^{\text{KP}}$  subgraph: This subgraph  $G^{\text{KP}} = (V^{\text{KP}}, E^{\text{KP}})$  represents the relationships between the control parameters and the KPIs. Nodes of  $G^{\text{KP}}$  are both the parameters and the KPIs, i.e.,  $V^{\text{KP}} = \mathcal{K} \cup \mathcal{P}$ , and edges  $E^{\text{KP}}$  represent whether or not a parameter is modifying the value of a KPI  $p \in \mathcal{P}$ . Any 2-tuple  $(k, p) \in \mathcal{K} \times \mathcal{P}$  is an edge of  $G^{\text{KP}}$ , i.e.,  $(k, p) \in E^{\text{KP}}$  if and only if KPI  $k$  is directly affected by a parameter  $p$ . This will cause an indirect conflict.

$G^{\text{P'P}}$  subgraph: This subgraph  $G^{\text{P'P}} = (V^{\text{P'P}}, E^{\text{P'P}})$  represents the relationships between the control parameters themselves. Nodes of  $G^{\text{P'P}}$  are both the parameters in the sets  $\mathcal{P}'$  and  $\mathcal{P}$ , i.e.,  $V^{\text{P'P}} = \mathcal{P}' \cup \mathcal{P}$ , and edges  $E^{\text{P'P}}$  represent whether or not a parameter  $p \in \mathcal{P}$  is modifying the value of another parameter  $p' \in \mathcal{P}'$ . Any 2-tuple  $(p', p) \in \mathcal{P}' \times \mathcal{P}$  is an edge of  $G^{\text{P'P}}$ , i.e.,  $(p', p) \in E^{\text{P'P}}$  if and only if a parameter  $p'$  is directly affected by a parameter  $p$ . This will cause an implicit conflict.

To construct the graph  $G^{\text{PA}}$ , the GSL iterates over the applications and the parameters nodes and stores their corresponding state values. Subsequently, the resultant graph nodes are xApps and the parameters. The edges represent the nodes having a state "1" concurrently. The edges reflect the nodes that are affecting each other at the same time. This leads to direct conflicts.

Similarly, to build the graph  $G^{\text{KP}}$ , the GSL iterates over the parameters and the KPIs nodes and stores their corresponding state values. The output graph nodes are the parameters and the KPIs. The edges indicate the parameters and KPIs whose values change simultaneously by having a state "1", resulting in implicit conflicts.

Lastly, to create the graph  $G^{\text{P'P}}$ , the GSL iterates over the parameters and checks their state values. The nodes of the graphs are the parameters, and the edges refer to the links among the parameters that have a state "1". This means the parameters are impacting each other behavior. This produces indirect conflicts.

During the construction of the three subgraphs, unique node

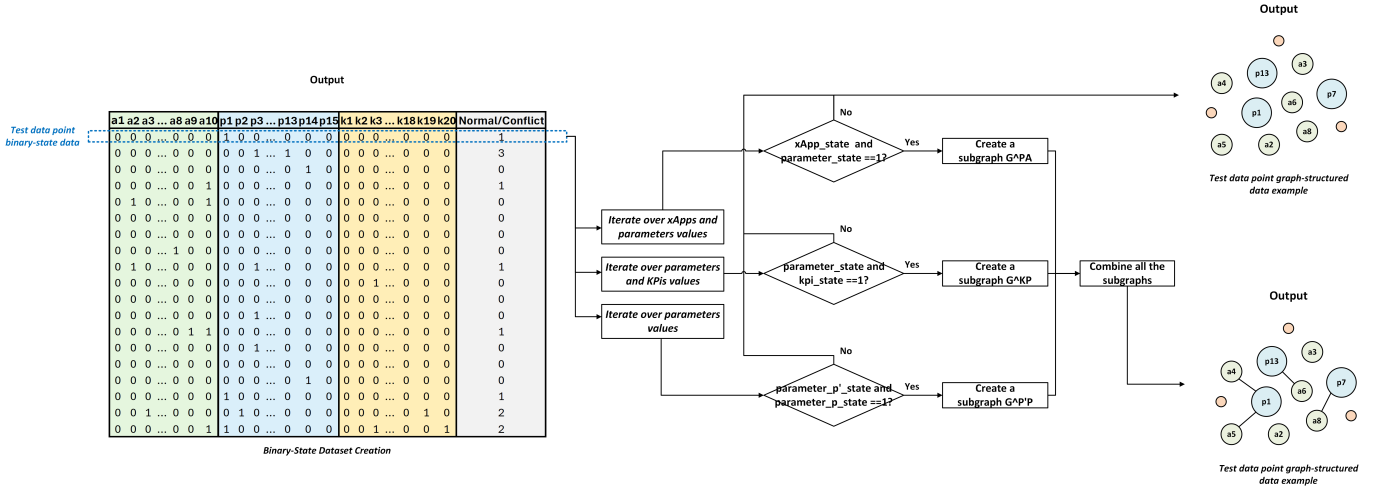


Fig. 5. The graph structure creator module steps.

features and edge attributes are assigned to the nodes and their edges that are contributing to the same type of conflict. GCN uses node features as the starting point to update the node embeddings (representations) through multiple layers of convolutions. These embeddings are refined iteratively as the model propagates information across neighboring nodes. Including edge attributes in the graph convolution process allows the model to learn a more nuanced understanding of node interactions. When performing convolution, edge attributes help the GCN understand the nature of the relationship between nodes.

### C. Graph Anomaly Detector (GAD)

The GAD module is responsible for detecting whether the instance is normal or whether we have a conflict (see Fig. 6). The output of GAD will be one of four labels (0: normal, 1: direct conflict, 2: implicit conflict, and 3: indirect conflict). The fully constructed graph structure from the GSL module is fed to the GAD module. It consists of a lightweight Graph Convolutional Network (GCN). GCN learns node-level representations from the graph-structured data, which are then aggregated via a global mean pooling into a graph-level representation for final classification. Then, a fully connected neural network (NN) layer is used to learn the final transformation from the graph's representation to the output classes.

To address the imbalances in the datasets, the classifier is enhanced by a focal loss function [24]. It is an enhancement to the standard cross-entropy loss by adding two key parameters, alpha and gamma. This function adjusts the loss contribution of easy and hard examples. It focuses more on hard-to-classify examples that are misclassified by the model. In parallel, it down-weights the loss associated with easy-to-classify examples. Alpha adjusts for class imbalance by balancing the weight between different classes. Gamma focuses the model on harder examples by reducing the loss for easy, well-classified examples. This helps to prevent the model from being overwhelmed by the majority class in imbalanced datasets and gives more attention to challenging instances. We

compute alpha using inverse class weights by calculating the inverse frequency of each class in the dataset. On the other hand, gamma is manually tuned for model optimization. The focal loss function for multi-class classification is given by:

$$\mathcal{L}_{\text{focal}} = - \sum_{c=1}^C \alpha_c (1 - p_{t_c})^\gamma \log(p_{t_c}) \quad (1)$$

where:

- $C$  is the number of classes.
- $p_{t_c}$  is the predicted probability for the true class  $c$ .
- $\alpha_c$  is the weighting factor for class  $c$ , which can help address class imbalance.
- $\gamma$  is the focusing parameter, which down-weights the loss for well-classified examples.

For each sample, this loss function is computed by summing the individual losses for each class, where only the true class  $c$  contributes to the loss.  $p_{t_c}$  is defined as the predicted probability for the true class.

The model consists of a two-layer GCN. GCN is a type of GNN designed specifically to operate on graph-structured data. It operates by propagating node features through the graph, aggregating information from a node's neighbors, and learning a new representation for each node. The process is typically iterative (layer-wise), with each layer performing a graph convolution operation.

After passing through two layers of graph convolution, the final node representations are passed through a fully connected layer to perform graph classification. A mean pooling mechanism is applied to the node features. It aggregates information into a graph-level representation before making the final classification.

Instead of processing the entire graph at once, mini-batch processing is executed. This involves processing smaller sub-graphs simultaneously, which helps reduce memory usage and computational time. Furthermore, a stratified K-Fold is implemented to ensure that each fold in the cross-validation process has a similar distribution of classes as the entire dataset during training and validation. This is particularly useful since



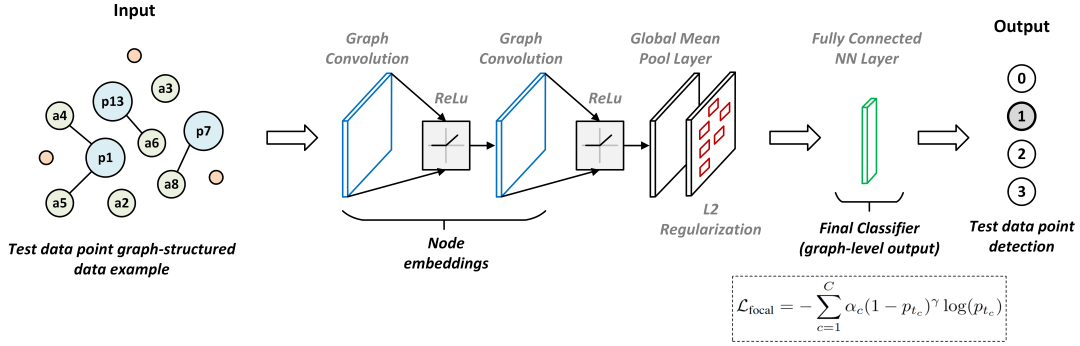


Fig. 6. The graph anomaly detector module steps.

our datasets are highly imbalanced. L2 regularization (also known as Ridge regularization) [25] is implemented by tuning the weight decay parameter. This helps to mitigate overfitting by adding a penalty to the loss function that prevents the model from giving too much weight to any single feature. It achieves this by squaring the model’s weights and adding the result to the loss, causing the model to prefer lower weight values. The equation for L2 regularization is given by:

$$\mathcal{L}_{L2} = \lambda \sum_{i=1}^n w_i^2 \quad (2)$$

where:

- $\lambda$  is the regularization parameter (also called the penalty term or weight decay), which controls the strength of the regularization.
- $w_i$  is the weight for the  $i$ -th feature in the model.
- $n$  is the total number of weights in the model.

#### D. Root Cause Analyst (RCA)

The RCA module is responsible for explaining the GAD module detections by providing the root causes (xApps) contributing to the detected conflicts (see Fig. 7). The detections from GAD and the whole constructed graph structure obtained from GSC are passed to the RCA module. The output is a subset of the graph of the detected conflicts.

The subset of the graph corresponding to each detection is further analyzed. In particular, it checks the source node with more than one incoming edge, as shown in Fig. 1. This means that the behavior of this node is being altered by more than one node. Then, it extracts the connected destination nodes as the root causes contributing to the detected conflict. The root causes are logged in a CSV file.

Addressing the root causes proactively improves long-term performance and system stability. A proactive approach relies on a deep understanding of the factors contributing to a problem. By analyzing data to uncover the root causes of service degradation in the network, mobile operators can make informed decisions to avoid reactive responses that are often incomplete or insufficient.

## IV. EXPERIMENTS AND RESULTS

This section presents the evaluation metrics, experimental setup, and performance metrics results of the proposed solution. The experimental setup outlines the environment, tools, and methodologies employed to assess the effectiveness of GRACE, while the results provide a comprehensive interpretation and analysis of its performance.

#### A. Experimental Setup

To evaluate the performance of our method, we use precision (Prec), recall (Rec) and F1-Score (F1) over the test dataset and its ground truth values:  $F1 = \frac{2 \times \text{Prec} \times \text{Rec}}{\text{Prec} + \text{Rec}}$ , where  $\text{Prec} = \frac{\text{TP}}{\text{TP} + \text{FP}}$  and  $\text{Rec} = \frac{\text{TP}}{\text{TP} + \text{FN}}$ . TP, TN, FP, and FN represent true positives, true negatives, false positives, and false negatives, respectively. Our generated datasets are highly imbalanced, which justifies the choice of these metrics that are suitable for imbalanced data.

We simulated and tested our model on an NVIDIA DGX station Intel(R) Xeon(R) CPU ES-2698 v4 @2.20GHz, 20core/40ht with 256GB of memory. The model is trained using the Adam optimizer with a learning rate of 0.01, the ReLU activation function, and a weight decay of 1e-4. The training process utilizes a batch size of 128, employing 5-fold cross-validation over 1,000 epochs. A two-layer GCN model is used to operate on the graph’s node features. It performs graph convolutions and aggregates information from the graph structure. Global mean pooling [26] is applied to return batch-wise graph-level-outputs by averaging node features across the node dimension.

#### B. Experiment Results

We conducted a parametric study provided by TABLE I to systematically investigate how  $\gamma$  value influences the model’s performance. The importance of this step lies in its ability to provide deeper insights into how  $\gamma$  contributes to the model’s behavior. Understanding this correlation allows us to make better-informed judgments during the optimization phase.

For the balanced dataset,  $\gamma$  is set to zero in the focal loss function as the classes are equally distributed. All the classes contribute similarly to the loss function and the model is less likely to be biased toward the majority class. There is no need to emphasize the harder examples or penalize the easier

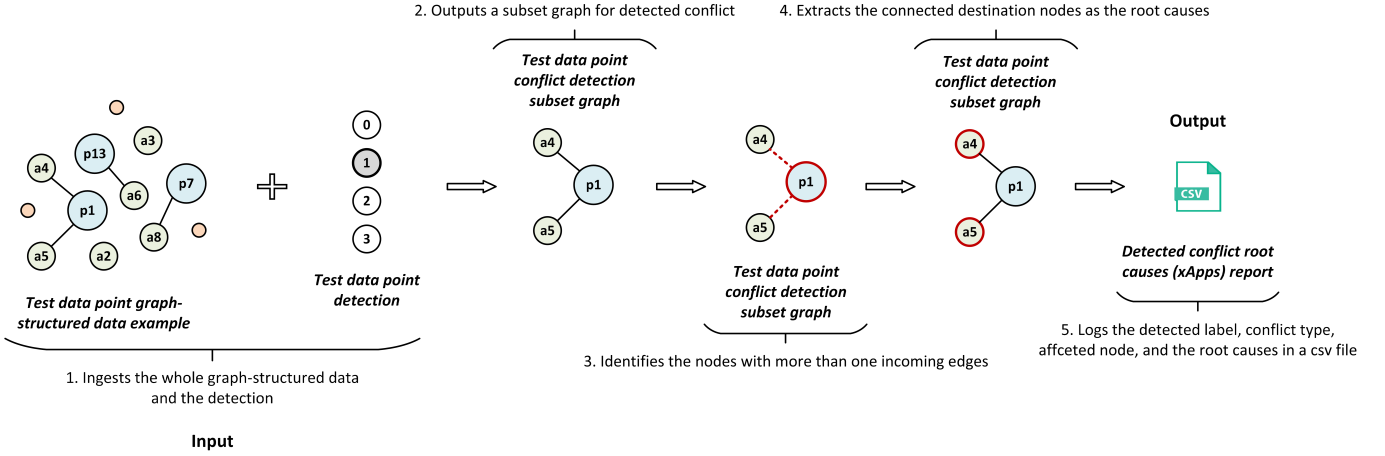


Fig. 7. The root cause analyst module steps.

ones. The model demonstrates significant performance on the balanced dataset, achieving high precision, recall, and F1 of 0.9829, 0.9818, and 0.9817, respectively.

We evaluated different  $\gamma$  values, ranging from 0.0 to 4.0, for the imbalanced datasets under investigation, as outlined in TABLE I. As the value of  $\gamma$  increases, the performance metrics improve until  $\gamma$  reaches 2.5 for the dataset with 40% conflict, where a high F1 of 0.9827 is achieved. Conversely, for the datasets with conflict percentages ranging from 30% to 10%, a  $\gamma$  value of 3.5 yields superior performance. Specifically, the F1 for these datasets are 0.9864, 0.9924, and 0.9912, respectively. After this point, the metrics values decrease. This reduction in performance is expected, as excessively high values of  $\gamma$  cause the model to overly focus on misclassified examples, potentially leading to overfitting. This, in turn, reduces the model's ability to generalize to easier examples, resulting in a decrease in overall performance.

The variation of the  $\gamma$  parameter significantly influences the model's performance. As  $\gamma$  increases, the model places greater emphasis on hard-to-classify examples, thereby enhancing recall by improving its ability to identify difficult or underrepresented cases. However, this focus on challenging examples can lead to a reduction in precision, as the model may misclassify some simpler instances. Conversely, when  $\gamma$  is set to a lower value, the model treats all examples with equal importance, resulting in a more balanced performance. However, this may limit the model's capacity to adequately focus on difficult cases. Therefore, selecting the optimal  $\gamma$  value is crucial for achieving a balance between precision and recall, ensuring the model performs effectively without overfocusing on any particular type of conflict.

The model exhibits high precision, recall, and F1 for the datasets under study, indicating its excellent performance in classifying data. The high precision indicates that when the model detects a positive class, it is correct most of the time, minimizing false positives. The high recall shows that the model is effective at identifying most of the true positive instances, reducing false negatives. The F1 demonstrates that the model achieves an outstanding balance between precision and

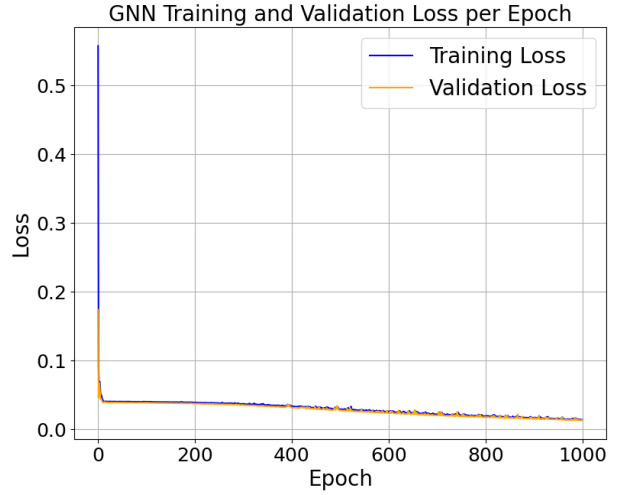


Fig. 8. GRACE training and validation loss per epoch on the 10% conflict dataset.

recall since it balances these two metrics. These findings imply that the model is accurate and reliable, correctly classifying the conflicts while avoiding significant classification errors.

The training and validation losses plot for the 10% conflict dataset ( $\gamma = 3.5$ ) is shown in Fig. 8. The losses decrease throughout training. This indicates that the model is effectively learning from the data over time. Initially, both losses were high. This reflects the model's early stage of learning, where it struggles to fit the data. As the training progresses, the loss decreases, indicating that the model is gradually learning to make better detections on the training data. Thus, the model improves its ability to fit the training data and gradually minimizes the error between its detections and the actual values. Similarly, the validation loss decreases, suggesting that the model is generalizing well and not overfitting to the training set. Both losses decrease at a similar rate and converge to a low value of less than 0.05. The trend of decreasing losses typically points to a well-optimized model, learning meaningful patterns and avoiding excessive complexity or bias.

TABLE I  
GCN PERFORMANCE IN DIFFERENT SETUPS

Datasets	Performance Metrics									
		$\gamma=0.0$	$\gamma=0.5$	$\gamma=1.0$	$\gamma=1.5$	$\gamma=2.0$	$\gamma=2.5$	$\gamma=3.0$	$\gamma=3.5$	$\gamma=4.0$
40% conflict	Prec	0.8892	0.9529	0.9592	0.9543	0.9755	0.9843	0.9546	0.9525	0.7242
	Rec	0.8686	0.9200	0.9486	0.9429	0.9714	0.9829	0.9429	0.9257	0.8000
	F1	0.8449	0.9139	0.9469	0.9392	0.9710	<b>0.9827</b>	0.9394	0.9183	0.7501
30% conflict	Prec	0.7831	0.8850	0.9428	0.9709	0.9699	0.9778	0.9818	0.9881	0.9755
	Rec	0.8267	0.8600	0.9267	0.9667	0.9600	0.9733	0.9800	0.9867	0.9733
	F1	0.7993	0.8394	0.9261	0.9642	0.9579	0.9723	0.9785	<b>0.9864</b>	0.9722
20% conflict	Prec	0.8526	0.8475	0.8925	0.9748	0.9805	0.9751	0.9469	0.9934	0.9047
	Rec	0.9000	0.8846	0.9231	0.9692	0.9769	0.9692	0.9385	0.9923	0.9077
	F1	0.8729	0.8460	0.9054	0.9656	0.9747	0.9658	0.9312	<b>0.9924</b>	0.9057
10% conflict	Prec	0.8486	0.8200	0.8183	0.8716	0.8810	0.9226	0.9240	0.9942	0.9382
	Rec	0.9035	0.9035	0.8947	0.9211	0.9386	0.9298	0.9474	0.9912	0.9298
	F1	0.8716	0.8704	0.8509	0.8916	0.9089	0.9162	0.9321	<b>0.9912</b>	0.9200

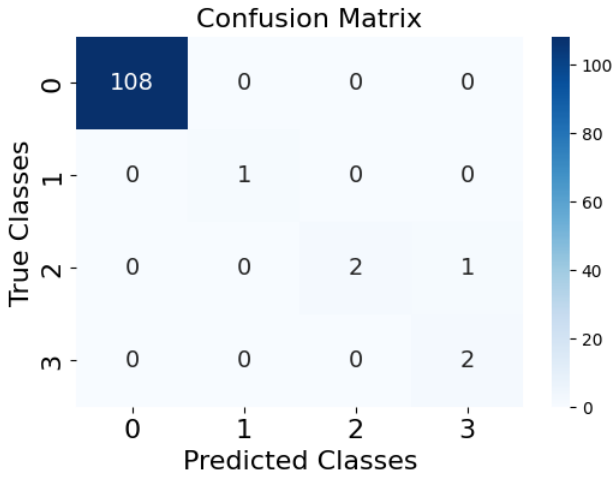


Fig. 9. GRACE testing confusion matrix on the 10% conflict dataset.

The confusion matrix (CM) of the proposed method testing on the 10% conflict dataset is elucidated in Fig. 9. CM provides a comprehensive overview of how well the model is performing by showing the number of the detected class and the true class. It allows us to identify if the model is biased toward the majority classes, especially in our case, where there are highly imbalanced datasets. The test set is composed of 114 instances. Out of the 114 instances, we have 108 normal, 1 direct conflict, 3 implicit conflicts (where 1 is misclassified as indirect conflict), and 2 indirect conflicts. By analyzing the figure, the diagonal elements of the matrix where the label and detected labels match are larger than the off-diagonal elements, which represent misclassifications. This indicates that the model can generalize well to new unseen data.

The conflict RCA report for the 10% conflict test dataset is illustrated in Fig. 10. The snapshot is filtered to show the detected conflict root causes. It indicates the detected label, the type of the conflict, the affected node, and the root causes (nodes and xApps). The affected node is the one whose behavior is altered by one or more nodes. The root causes nodes are the nodes that are concurrently modifying

Detected Label	Normal/Conflict	Affected Node	Root Causes Nodes
1	Direct	p7	a4, a7
2	Implicit	k10	p1, p9
2	Implicit	k5	p4, p2
3	Indirect	p8	p11, p15
3	Incorrect Detection		
3	Indirect	p6	p2, p8

Fig. 10. Conflicts RCA report for the 10% conflict dataset.

the same node. The root causes (xApps) are the xApps that are contributing to the detected conflict. The first line of the report shows a direct conflict occurrence (the detected label is 1) between two xApps (a4, and a7). In particular, these two applications control the same parameter p7. Thus, the root causes of this detected direct conflict are a4, and a7.

The experimental results validate the performance of our proposed model which is a great candidate to address highly imbalanced datasets. The model demonstrates strong generalization capabilities, making it well-suited for practical application in real-world scenarios.

## V. CONCLUSION

In this work, we proposed a novel data-driven GCN-based method called GRACE for xApps conflict management and RCA in O-RAN. GRACE takes a binary-state dataset as input for the xApps, parameters, and KPIs in the network and constructs graph-structured data. Subsequently, it leverages GCN with a focal loss function to detect the occurrence of three types of conflicts (direct, indirect, and implicit). The learned graph structure and the detections are exploited to determine the root causes (xApps) that are contributing to the detected conflicts. The model demonstrates exceptional performance on highly imbalanced datasets. With conflicts ranging from 40% to 10%, the proposed model achieves a high F1 score greater than 98% on various evaluation metrics. Future work will focus on developing predictive maintenance



with mitigation strategies based on the retrieved root causes to prevent performance degradation and reduce xApp conflicts across multi-vendor environments. Additionally, we plan to deploy and test the model in a real-life environment to further enhance its performance and applicability.

## REFERENCES

- [1] M. Polese, L. Bonati, S. D’Oro, S. Basagni, and T. Melodia, “Understanding o-ran: Architecture, interfaces, algorithms, security, and research challenges,” *IEEE Communications Surveys & Tutorials*, vol. 25, no. 2, pp. 1376–1411, 2023.
- [2] B. Balasubramanian, E. S. Daniels, M. Hiltunen, R. Jana, K. Joshi, R. Sivaraj, T. X. Tran, and C. Wang, “Ric: A ran intelligent controller platform for ai-enabled cellular networks,” *IEEE Internet Computing*, vol. 25, no. 2, pp. 7–17, 2021.
- [3] L. Bonati, S. D’Oro, M. Polese, S. Basagni, and T. Melodia, “Intelligence and learning in o-ran for data-driven nextg cellular networks,” *IEEE Communications Magazine*, vol. 59, no. 10, pp. 21–27, 2021.
- [4] M. Wani, M. Kretschmer, B. Schröder, A. Grebe, and M. Rademacher, “Open ran: A concise overview,” *IEEE Open Journal of the Communications Society*, vol. 6, pp. 13–28, 2025.
- [5] R. Ntassah, G. M. Dell’Aera, and F. Granelli, “xapp for traffic steering and load balancing in the o-ran architecture,” in *ICC 2023 - IEEE International Conference on Communications*, 2023, pp. 5259–5264.
- [6] D. Anand, M. A. Togou, and G.-M. Muntean, “Enhancing qoe diversity in hetnets through interference mitigation with ml-based xapp in a 5g o-ran architecture,” in *ICC 2024 - IEEE International Conference on Communications*, 2024, pp. 5473–5478.
- [7] B. H. Prananto, Iskandar, Hendrawan, and A. Kurniawan, “Lstm neural network algorithm for handover improvement in a non-ideal network using o-ran near-rt ric,” *IEICE Transactions on Communications*, vol. E107-B, no. 6, pp. 458–469, 2024.
- [8] P. Cumino, J. Baranda, M. Luis, D. Rosario, E. Cerqueira, J. Mangués, and S. Sargento, “Enhancing mobile network performance through oran-integrated uav-based mobility management,” in *IEEE INFOCOM 2024 - IEEE Conference on Computer Communications Workshops (INFOCOM WKSHPS)*, 2024, pp. 1–8.
- [9] C. Adamczyk, “Challenges for conflict mitigation in o-ran’s ran intelligent controllers,” in *2023 International Conference on Software, Telecommunications and Computer Networks (SoftCOM)*. IEEE, 2023, pp. 1–6.
- [10] H. Zafar, E. Tohidi, M. Kasparick, B. Lorbeer, H. Lehmann, M. Weh, G. Rastogi, J. Charaf, M. Tarwala, A. Kliks *et al.*, “Ric-apps conflict management,” i14y Lab, Tech. Rep., 2024.
- [11] M. Hoffmann, S. Janji, A. Samorzewski, L. Kułacz, C. Adamczyk, M. Dryjański, P. Kryszkiewicz, A. Kliks, and H. Bogucka, “Open ran xapps design and evaluation: Lessons learnt and identified challenges,” *IEEE Journal on Selected Areas in Communications*, vol. 42, no. 2, pp. 473–486, 2024.
- [12] M. Polese, L. Bonati, S. D’Oro, S. Basagni, and T. Melodia, “Colo-ran: Developing machine learning-based xapps for open ran closed-loop control on programmable experimental platforms,” *IEEE Transactions on Mobile Computing*, vol. 22, no. 10, pp. 5787–5800, 2023.
- [13] A. Lacava, M. Polese, R. Sivaraj, R. Soundrarajan, B. S. Bhati, T. Singh, T. Zugno, F. Cuomo, and T. Melodia, “Programmable and customized intelligence for traffic steering in 5g networks using open ran architectures,” *IEEE Transactions on Mobile Computing*, vol. 23, no. 4, pp. 2882–2897, 2024.
- [14] M. Huang and J. Chen, “Proactive mobility load balancing through interior-point policy optimization for open radio access networks,” *IEEE Transactions on Mobile Computing*, vol. 24, no. 2, pp. 500–506, 2025.
- [15] J. Dai, L. Li, R. Safavinejad, S. Mahboob, H. Chen, V. V. Ratnam, H. Wang, J. Zhang, and L. Liu, “O-ran-enabled intelligent network slicing to meet service-level agreement (sla),” *IEEE Transactions on Mobile Computing*, vol. 24, no. 2, pp. 890–906, 2025.
- [16] H. Zhang, H. Zhou, and M. Erol-Kantarci, “Team learning-based resource allocation for open radio access network (o-ran),” in *ICC 2022 - IEEE International Conference on Communications*, 2022, pp. 4938–4943.
- [17] A. Wadud, F. Golpayegani, and N. Afraz, “Conflict management in the near-rt-ric of open ran: A game theoretic approach,” in *2023 IEEE International Conferences on Internet of Things (iThings) and IEEE Green Computing & Communications (GreenCom) and IEEE Cyber, Physical & Social Computing (CPSCom) and IEEE Smart Data (SmartData) and IEEE Congress on Cybermatics (Cybermatics)*. IEEE, 2023, pp. 479–486.
- [18] —, “Qacm: Qos-aware xapp conflict mitigation in open ran,” *IEEE Transactions on Green Communications and Networking*, vol. 8, no. 3, pp. 978–993, 2024.
- [19] H. Erdol, X. Wang, R. Piechocki, G. Oikonomou, and A. Parekh, “xapp distillation: Ai-based conflict mitigation in b5g o-ran,” *arXiv preprint arXiv:2407.03068*, 2024.
- [20] P. B. del Prever, S. D’Oro, L. Bonati, M. Polese, M. Tsampazi, H. Lehmann, and T. Melodia, “Pacifista: Conflict evaluation and management in open ran,” *arXiv preprint arXiv:2405.04395*, 2024.
- [21] A. Zolghadr, J. F. Santos, L. A. DaSilva, and J. Kibilda, “Learning and reconstructing conflicts in o-ran: A graph neural network approach,” *arXiv preprint arXiv:2412.14119*, 2024.
- [22] J. Armstrong, E. Fallon, and S. Fallon, “Pre-emptive conflict detection architecture for o-ran service management and orchestration,” in *2024 IEEE International Conference on Industry 4.0, Artificial Intelligence, and Communications Technology (IAICT)*, 2024, pp. 335–340.
- [23] A. Sultana, F. Bashar, M. R. Chowdhury, and A. P. Da Silva, “A software-defined radio based o-ran platform for xapp conflict detection and mitigation,” in *MILCOM 2024 - 2024 IEEE Military Communications Conference (MILCOM)*, 2024, pp. 686–687.
- [24] T.-Y. Ross and G. Dollár, “Focal loss for dense object detection,” in *proceedings of the IEEE conference on computer vision and pattern recognition*, 2017, pp. 2980–2988.
- [25] A. E. Hoerl and R. W. Kennard, “Ridge regression: Biased estimation for nonorthogonal problems,” *Technometrics*, vol. 12, no. 1, pp. 55–67, 1970.
- [26] R. Aljundi, G. Farquhar, E. Ricci, S. Maskell, S. Shah, A. Javed, M. Besserve, T. Cohn, and M. Defferrard, “Graph u-nets,” in *Proceedings of the 36th International Conference on Machine Learning (ICML)*, 2019. [Online]. Available: <https://arxiv.org/abs/1905.05178>

**Maryam Al Shami** (Women in Engineering Member, IEEE) is a PhD candidate at Concordia Institute for Information Systems Engineering, Montreal, QC, Canada. Her current research focus is on proactive network management and root cause analysis in 5G RAN and beyond. Her research interests include 5G Networks and Beyond, Self-Healing Networks, Explainable AI/ML, Causal Discovery, Root Cause Analysis, and Predictive Maintenance.

**Jun Yan** (Member, IEEE) is the Concordia University Research Chair (Tier 2) in Artificial Intelligence in Cyber Security and Resilience and an Associate Professor at Concordia Institute for Information Systems Engineering, Montreal, QC, Canada. His research interests include Cyber-physical systems and security, applied and adversarial computational intelligence, smart grids, smart transportation, smart cities, and attack-resilient systems and control.

**Emmanuel Thepie Fapi** is a Senior Data Scientist at Ericsson Canada, AI Hub Canada, Montreal. Prior to Ericsson, he worked as a Software Developer with Amazon Lab126, QNX Software System Limited, GENBAND U.S. LLC, MDA Systems, and Easy G. He holds a PhD from IMT Atlantique in signal processing and telecommunications in Brest, France. He also received a master’s degree in engineering mathematics and computer tools from Orleans University in France. His research interests are 5G Networks and Beyond, Distributed AI/ML, Edge Computing, Autonomous Vehicles, Sustainable AI, Trustworthy AI, Non-Terrestrial Networks, Zero-Trust Architecture, Embedded Systems, and Advanced Digital Signal Processing.